Multiredox Heterometallic Carbosilane Dendrimers

Magdalena Zamora, Beatriz Alonso, César Pastor, and Isabel Cuadrado*

Departamento de Química Inorgánica, Facultad de Ciencias, Universidad Autónoma de Madrid, Cantoblanco, 28049, Madrid, Spain

Received June 8, 2007

A convergent growth approach for the synthesis of novel heterometallic dendritic molecules derived from carbosilane frameworks and functionalized with silicon-bridged ferrocenyl and (η^6-aryl)tricarbonylchromium moieties has been developed. The synthetic route involves the construction of the dendritic fragments (CH_2═CH)MePhSiFc (**1**) (Fc = (η^5-C_5H_4)Fe(η^5-C_5H_5)) (CH_2═$CHCH_2$)PhSi[$(CH_2)_2$MePhSiFc]$_2$ (**3**), (CH_2═CH)MeSi[{(η^6-C_6H_5)Cr($CO)_3$}Fc] (**4**), and (CH_2═$CHCH_2$){(η^6-C_6H_5)Cr($CO)_3$}MeSi[$(CH_2)_2$-Me{(η^6-C_6H_5)Cr($CO)_3$}SiFc]$_2$ (**5**), containing a single reactive C═C functionality, in addition to ferrocenyl (**1** and **3**) and linked ferrocenyl and (η^6-C_6H_5)Cr($CO)_3$ moieties (**4** and **5**) and their subsequent attachment to the tetrafunctional core Si[$(CH_2)_3$Si$(Me)_2H]_4$ (**6**), via platinum-catalyzed hydrosilylation reactions. The first- and second-generation dendrimers **8** and **9**, containing four and eight ferrocenyl units on the dendritic surface, respectively, have been prepared by this procedure. Thermal treatment of **8** and **9** with Cr$(CO)_6$ afforded the targeted heterometallic dendrimers **7** and **10**, carrying silicon-bridged (η^5-C_5H_4)Fe(η^5-C_5H_5) and (η^6-C_6H_5)Cr($CO)_3$ moieties appended at the dendrimer periphery. The molecular structures of the vinyl-functionalized silanes **1** and **4** have been determined by single-crystal X-ray diffraction. The crystal structure of **4** showed that the Cr$(CO)_3$ group is disposed in a *transoid* configuration with respect to the ferrocenyl moiety. The heterobimetallic **4** also shows an interesting self-assembly of the metals (Fe and Cr) in the crystal. The electrochemical behavior of all new dendritic molecules has been investigated. For the heterometallic **4**, **7**, and **10** the oxidation of the iron centers becomes more anodic compared to the oxidation of the ferrocenyl units in the homometallic molecules **1**, **8**, and **9**, due to the electron-withdrawing nature of the neighboring silicon-linked (η^6-C_6H_5)Cr($CO)_3$ moieties. In addition, stable electrode surfaces modified with dendrimers **8** and **9** have been prepared.

Introduction

One of the most significant recent highlights in the field of dendrimer chemistry[1] lies in the incorporation of transition metals into dendritic structures to create metallodendrimers, which offers many additional possibilities for applications as functional materials with interesting electrochemical, catalytic, photo-optical, and magnetic properties.[2,3] A challenging target is the possibility to insert a controlled number of different organometallic centers in predetermined sites of the dendritic structure. The presence of two (or more) different metal centers within the same dendritic molecule can profoundly affect both the physical properties and the reactivity of the dendritic system. It is thus possible to construct heterometallic dendrimers capable of performing complex functionality resulting from the integration of the specific properties of their dissimilar constituent organometallic moieties. This may result in the development of a variety of novel and improved characteristics that do not occur in homometallic dendritic molecules. Although synthetic methods for homometallic dendrimers are well developed,[2,3] synthetic efforts for the construction of dendritic molecules containing two or more different organotransition metal moieties are limited, and only a few attempts have been made in this direction.[4−9] In particular, metallodendrimers having two different redox-active organometallic units are systems of intrinsic interest, as each of the chemically different organometallic units introduces into the same dendritic structure its own ability to

* Corresponding author. E-mail: isabel.cuadrado@uam.es. Tel: (+34) 91 397 4834. Fax: (+34) 91 397 4833.

(1) See for example: (a) Newkome, G. R., Moorefield, C. N., Vögtle, T., Eds.; *Dendrimers and Dendrons: Concept, Syntheses and Applications*; Wiley-VCH Verlag: Weinheim, Germany, 2001. (b) Frechét, J. M. J., Tomalia, D. A., Eds.; *Dendrimers and Other Dendritic Polymers*; VCH: Weinheim, Germany, 2002. (c) Vögtle, F.; Gestermann, S.; Hesse, R.; Schwierz, H.; Windisch, B. *Prog. Polym. Sci.* **2000**, *25*, 987. (d) Tomalia, D. A. *Prog. Polym. Sci.* **2005**, *30*, 294.

(2) For metallodendrimers, see for example: (a) Newkome, G. R.; Moorefield, C. N. *Chem. Rev.* **1999**, *99* 1689. (b) Gorman, C. *Adv. Mater*. **1998**, *10*, 295. (b) Majoral, J.-P.; Caminade, A.-M. *Chem. Rev.* **1999**, *99*, 845. (c) *Metal-Containing and Metallosupramolecular Polymers and Materials*; Schubert, U. S., Newkome, G. R., Manners, I., Eds.; Oxford University Press: London, 2006. (d) Mery, D.; Astruc, D. *Coord. Chem. Rev.* **2006**, *250*, 1965. (e) Berger, A.; Gebbink, R. J. M.; van Koten, G. *Top. Organomet. Chem*. **2006**, *20*, 1. (f) Newkome, G. R. In *Frontiers in Transition Metal-Containing Polymers*; Abd-El-Aziz, A. S. A, Manners, I., Eds.; Wiley: Hoboken, NJ, 2007; Chapter 10.

(3) For reviews on organometallic dendrimers, see for example: (a) Cuadrado, I.; Morán, M.; Casado, C. M.; Alonso, B.; Losada, J. *Coord. Chem. Rev.* **1999**, *193*−*195*, 395. (b) Hearshaw, M. A.; Moss, J. R. *Chem. Commun.* **1999**, 1. (c) Rossell, O.; Seco, M.; Angurell, I. *C. R. Chim.* **2003**, *6*, 805. (d) Chase, P. A.; van Koten, G. *J. Organomet. Chem.* **2004**, *689*, 4016. (e) Manners, I. In *Synthetic Metal-Containing Polymers*; Manners, I., Ed.; Wiley-VCH: Weinheim, 2004; p 237. (f) Astruc, D. In *Frontiers in Transition Metal-Containing Polymers*; Abd-El-Aziz, A. S. A., Manners, I., Eds.; Wiley: Hoboken, NJ, 2007; Chapter 11.

(4) (a) Angurell, I.; Rossell, O.; Seco, M.; Ruiz, E. *Organometallics* **2005**, *24*, 6365. (b) Angurell, I.; Lima, J. C.; Rodriguez, L.-I.; Rossell, O.; Seco, M. *New J. Chem.* **2006**, *30*, 1004.

(5) Méry, D.; Plault, L.; Ornelas, C.; Ruiz, J.; Nlate, S.; Astruc, D.; Blais, J.-C.; Rodrigues, J.; Stéphane, C.; Kiracki, K.; Perrin, C. *Inorg. Chem*. **2006**, *45*, 1156.

(6) Casado, C. M.; González, B.; Cuadrado, I.; Alonso, B.; Morán, M.; Losada, J. *Angew. Chem., Int. Ed*. **2000**, *39*, 2135.

(7) Achar, S.; Immoos, C. E.; Hill, M. G.; Catalano, V. J. *Inorg. Chem*. **1997**, *36*, 2314.

(8) Liu, G. X.; Puddephatt, R. J. *Organometallics* **1996**, *15*, 5257.

(9) Juris, A.; Balzani, V.; Campagna, S.; Denti, G.; Serroni, S.; Frei, G.; Guedel, H. U. *Inorg. Chem*. **1994**, *33*, 1491.

10.1021/om700559t CCC: $37.00
Publication on Web 09/15/2007

undergo redox processes at a certain potential. Therefore, these metallodendrimers can be used to perform valuable functions such as reversible exchange (storage and release) of a controlled number of electrons at a certain potential, an attractive characteristic for the design of molecular electronic devices and multi-electron-transfer catalysts.[10] Furthermore, such heterometallic dendrimers offer the unique opportunity to explore the dependence of electronic cooperativity on redox asymmetry and of chemical reactivity upon the presence of a second, different redox center in the same metallodendritic molecule. In this context, we have reported metallodendrimers containing neutral ferrocene and cationic cobaltocenium units located simultaneously at the surface of a dendritic structure.[6] These heterometallic dendrimers are of significance because they exhibit a double function. Thus, conducting films of electrodeposited dendrimers containing both ferrocene and cobaltocenium units have been used successfully in a double way for the aerobic and anaerobic determination of glucose.[11]

On the other hand, in the last years we have been exploring routes for the construction of new families of redox-active organometallic dendritic structures, containing nitrogen- and silicon-based frameworks.[12−15] One of our synthetic approaches to the synthesis of such organometallic macromolecules was based on hydrosilylation reactions that exploit the reactivity of Si−H polyfunctionalized carbosilanes and siloxanes toward suitable ferrocenyl derivatives containing reactive vinyl or allyl groups.[13−15] In this way, we have reported the first examples of organometallic dendritic molecules possessing peripheral electronically communicated ferrocenyl moieties, which were constructed using a convergent methodology by sequences of hydrosilylation and alkenylation reactions.[14,15] Our objective now is to extend this synthetic strategy to new dendritic molecules containing a controlled number of different electroactive organometallic units, precisely located in the dendritic structure. As a continuation of our efforts toward the development of new families of redox-active organometallic dendrimers, we have chosen now to combine in a dendritic molecule a typical strong electron-donating fragment such as ferrocene together with the electron-withdrawing moiety η^6-aryltricarbonylchromium.

We report herein full details on the synthesis, characterization, and redox behavior of a series of novel redox-active multimetallic dendritic systems, derived from carbosilane frameworks, containing ferrocenyl and $(\eta^6\text{-}C_6H_5)Cr(CO)_3$ moieties linked together in close proximity by a bridging silicon atom.

Results and Discussion

Synthesis of the Homo- and Heterometallic Precursor Dendritic Fragments 1−5. We are interested in developing methods for the synthesis of new redox-active silicon-based heterometallic dendritic molecules based on the convergent methodology.[16,17] In our designed convergent approach, suitable organometallic dendritic wedges containing a C═C functionality at the focal point are constructed first, and then these dendrons are attached to a Si−H polyfunctionalized core molecule via hydrosilylation chemistry in the final steps of the dendrimer construction.[14]

There were several key requirements that had to be met by the starting redox-active organometallic molecule in our convergent methodology. These considerations are based on our foreknowledge that organometallic dendrimer synthesis is inherently labor intensive, which involves lengthy and difficult synthetic steps and requires relatively large quantities of readily accessible starting organometallic materials.[18] Our prerequisites therefore call for a polyfunctional organometallic molecule that meets all the following criteria: (i) be easy to prepare; (ii) bear a single reactive C═C functionality appropriate for dendritic convergent growth; (iii) have tolerance to the conditions necessary for carbosilane chemistry (in particular, hydrosilylation conditions and inertness to Grignard reagents); (iv) carry a potential ligand binding site for attachment of a second different organotransition metal fragment; (v) this second organometallic moiety must to be incorporated without decomplexing the first starting organotransition metal fragment. With this in mind, the target redox-active precursor molecule was chosen to be the novel derivative ferrocenylmethylphenylvinylsilane (**1**), shown in Scheme 1.

The pivotal molecule **1** was easily accessible by the salt elimination reaction of ferrocenyllithium with methylphenylvinylchlorosilane in THF at −30 °C (Scheme 1). For this purpose (tri-*n*-butylstannyl)ferrocene was selected as starting material, since it has proved to be an excellent precursor of pure monolithioferrocene[19] (see Experimental Section). This is crucial, in order to exclude the formation of the dimetalated ferrocene, $Fe(\eta^5\text{-}C_5H_4Li)_2$, which could produce undesirable additional disubstituted dendritic materials. After appropriate workup, the target vinyl-terminated **1** was isolated in high purity and reasonable yield (75%) as an orange, crystalline solid. This simple organometallic molecule features several key components that meet the requirements detailed above. First, the reactive vinyl group attached to the silicon atom of **1** enables further elaboration via hydrosilylation reaction with Si−H polyfunctionalized building blocks in order to provide either a branched second-generation dendron or a first-generation final dendrimer in a typical convergent dendrimer growth. Second, the free aryl ring can be readily coordinated to a second different organotransition metal moiety via π-interaction. In addition, the redox-active **1** is thermally and air stable and soluble in common organic solvents. In fact, **1** can be stored for a long period (several months) under an air atmosphere at room temperature without noticeable decomposition (^{1}H NMR spectroscopy).

The convergent growth of the ferrocenyl derivative **1** was achieved by hydrosilylation reaction with phenylchlorosilane

(10) (a) *Supramolecular Electrochemistry*; Kaifer, A. E., Gómez-Kaifer, M., Eds.; Wiley-VCH: Weinheim: Germany, 1999; Chapter 16, p 207. (b) *Inorganic Electrochemistry. Theory, Practice and Application*; Zanello, P., Ed.; Royal Society of Chemistry: Cambridge, 2003; Chapter 5, p 185. (c) Astruc, D.; Daniel, M. C.; Nlate, S.; Ruiz, J. In *Trends in Molecular Electrochemistry*; Pombeiro, A. J. L., Amatore, C., Eds.; Marcel Dekker: New York, 2004; Chapter 9, p 283.

(11) Alonso, B.; García-Armada, P.; Losada, J.; Cuadrado, I.; González, B.; Casado, C. M. *Biosens. Bioelectron.* **2004**, *19*, 1617.

(12) (a) Cuadrado, I.; Morán, M.; Casado, C. M.; Alonso, B.; Lobete, F.; García, B.; Ibisate, M.; Losada, J. *Organometallics* **1996**, *15*, 5278. (b) Gonzalez, B.; Casado, C. M.; Alonso, B.; Cuadrado, I.; Morán, M.; Wang, Y.; Kaifer, A. E. *Chem. Commun.* **1998**, 2569. (c) Zamora, M.; Herrero, S.; Losada, J.; Cuadrado, I.; Casado, C. M.; Alonso, B. *Organometallics* **2007**, *26*, 2688.

(13) (a) Alonso, B.; Cuadrado, I.; Morán, M.; Losada, J. *J. Chem. Soc., Chem. Commun.* **1994**, 2575. (b) Alonso, B; Morán, M; Casado, C. M.; Lobete, F.; Losada, J.; Cuadrado, I. *Chem. Mater.* **1995**, *7*, 1440. (c) García, B.; Casado, C. M.; Cuadrado, I.; Alonso, B.; Morán, M.; Losada, J. *Organometallics* **1999**, *18*, 2349.

(14) Cuadrado, I.; Casado, C. M.; Alonso, B.; Morán, M.; Losada, J.; Belsky, V. *J. Am. Chem. Soc.* **1997**, *119*, 7613.

(15) Alonso, B.; González, B.; Ramírez, E.; Zamora, M.; Casado, C. M.; Cuadrado, I. *J. Organomet. Chem.* **2001**, *637−639*, 642.

(16) (a) Hawker, C. J.; Fréchet, J. M. J. *J. Chem. Soc., Chem. Commun.* **1990**, 1010. (b) Hawker, C. J.; Frechet, J. M. J. *J. Am. Chem. Soc.* **1990**, *112*, 7638.

(17) For an excellent recent review on convergent construction of dendrimers see: Grayson, S. K.; Fréchet, J. M. J. *Chem. Rev.* **2001**, *101*, 3819.

(18) Zamora, M. Ph.D. Thesis, Universidad Autónoma de Madrid, 2006.

(19) Guillaneux, D.; Kagan, H. B. *J. Org. Chem.* **1995**, *60*, 2502.

Scheme 1. Synthesis of the Homo- and Heterometallic Dendritic Fragments 1−5[a]

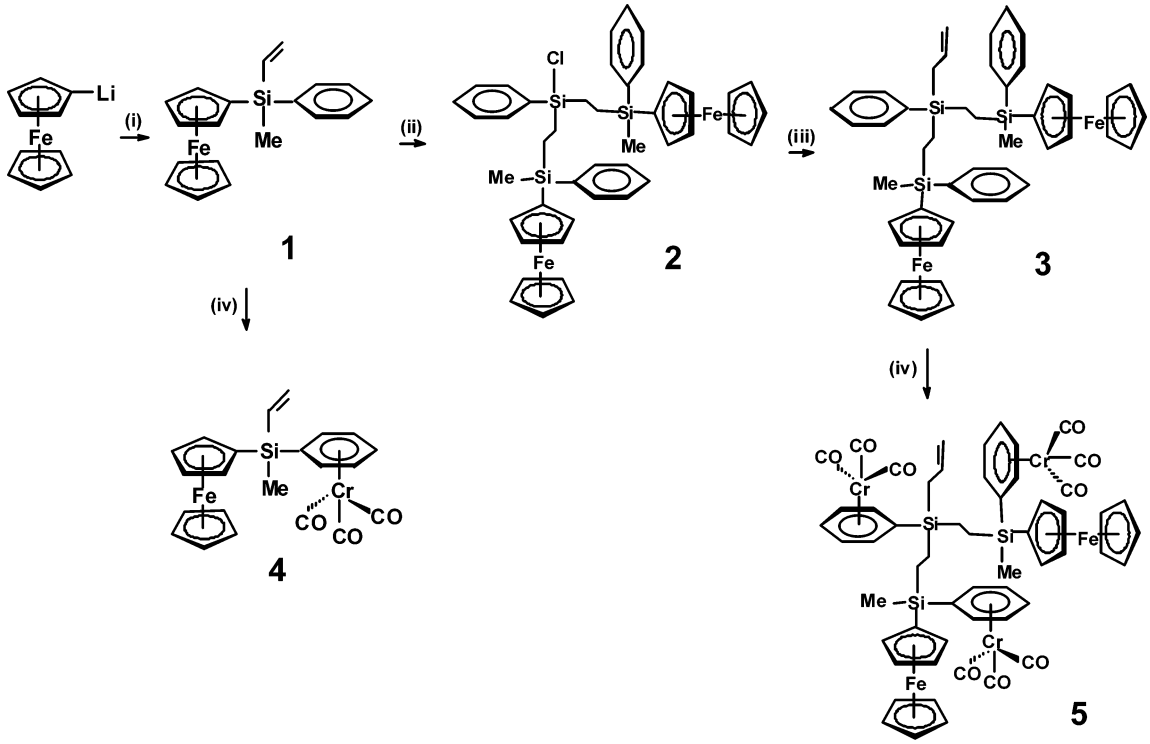

[a] Reagents and conditions: (i) $ClSiPhMe(CH{=}CH_2)$, THF, −30 °C; (ii) $ClSiPhH_2$, toluene, 40 °C, Karstedt's cat.; (iii) $(CH_2CH{=}CH_2)MgBr$, Et_2O, reflux; (iv) $Cr(CO)_6$, *n*-Bu_2O/THF (9:1, v/v), reflux.

in toluene at 40 °C in the presence of Karstedt's catalyst (Scheme 1). ^{1}H NMR and IR spectroscopies were utilized to follow the progress of the reaction, and it was established that complete reaction of the two Si−H functionalities of phenylchlorosilane was easily achieved under these mild conditions. The intermediate compound **2** was isolated as an orange, moisture-sensitive, oily product. The ^{1}H NMR spectrum of **2** evidences that only the β-isomer was formed under the described reaction conditions and no Markownikow addition (which would lead to α-isomer) took place,[20] which assures a regular dendritic convergent growth and the generation of molecules of maximum symmetry. Subsequent treatment of the terminal Si−Cl functionality in **2** with allylmagnesium bromide, followed by hydrolytic workup and purification via column chromatography, afforded an orange solid, which was isolated and characterized as being the desired growth dendron fragment **3** shown in Scheme 1, carrying two ferrocenyl units linked to phenyl rings by a bridging silicon atom.

The π-coordinating ability of the free phenyl rings of **1** and **3** toward transition metals offered a good chance to gain an easy synthetic access to the targeted first- and second-generation heterometallic dendrons. Thus, thermal treatment of **1** and **3** with $Cr(CO)_6$ in the donor solvent medium of *n*-dibutyl ether/tetrahydrofuran (9:1, v/v) at 140 °C afforded the heterobimetallic **4** and the heteropentametallic **5**, respectively (see Scheme 1). ^{1}H NMR spectroscopy was used to follow the progress of these reactions, by monitoring the considerable upfield shift of the aryl proton resonances upon coordination to the $Cr(CO)_3$ group. After these reactions were finished, it is necessary to remove some insoluble decomposition materials by filtration through a short column of Celite, resulting in bright yellow-orange solutions. The novel heterobimetallic dendrons **4** and **5** were isolated as yellow-orange crystals. The solids **4** and **5** may be handled in air for short periods of time, but the solutions must be handled under an inert atmosphere.

The structural identities of the novel dendritic molecules **1**−**5** were straightforwardly established on the basis of elemental analysis, IR, and multinuclear (^{1}H, ^{13}C, ^{29}Si) NMR spectroscopy and mass spectrometry. ^{1}H NMR spectra of **1**−**5** show in all cases the pattern of resonances centered at about δ 4.0 and 4.3 ppm, respectively, characteristic of the unsubstituted and substituted cyclopentadienyl ligands in the ferrocenyl moieties. The ^{1}H NMR spectra of **1** and **4** show a set of resonances characteristic of the reactive vinyl group at δ 5.9, 6.2, and 6.4 ppm in the expected integration ratios. Likewise, the three signals of the allyl part in **3** and **5** include two multiplets for each of $=CH_{(trans)}$ and $=CH_{(cis)}$ and a doublet at 1.9 ppm for the methine proton. In addition, in the ^{1}H NMR spectra of the heterometallics **4** and **5** the complete η^6-coordination of the $Cr(CO)_3$ moieties to the phenyl rings in the homometallic **1** and **3** was confirmed by the total absence of resonances in the range 7.3−7.5 ppm, in which the aryl resonances of the noncoordinated dendritic wedge are observed. As a consequence of the withdrawal of the π-electrons from the aryl rings by the $Cr(CO)_3$ moieties, the aromatic protons on the complexed dendrimer resonate at significantly higher field, in the region from 5.1 to 5.5 ppm. For both heterometallic molecules **4** and **5** additional evidence for the η^6-coordination of the $Cr(CO)_3$ group to the phenyl ring included the presence of the two typical ν-(C≡O) strong bands near 1970 and 1870 cm^{-1} in the IR spectra, related to the A_1 and E vibration modes of the $Cr(CO)_3$ tripod. The structures of **4** and **5** were also confirmed by the ^{13}C NMR spectra, which display exclusively the resonances expected for the different carbon atoms, with the characteristic upfield shift of ca. 37 ppm in the resonances of the coordinated aryl carbon nuclei relative to the uncoordinated aromatics of the ferrocenyl

(20) (a) *Comprehensive Handbook on Hydrosilylation*; Marciniec, B., Ed.; Pergamon Press: Oxford, 1992. (b) Ojima, I. In *The Chemistry of Organic Silicon Compounds*; Patai, S., Rappoport, Z., Eds.; John Wiley & Sons: New York, 1989; Part 2, p 1479.

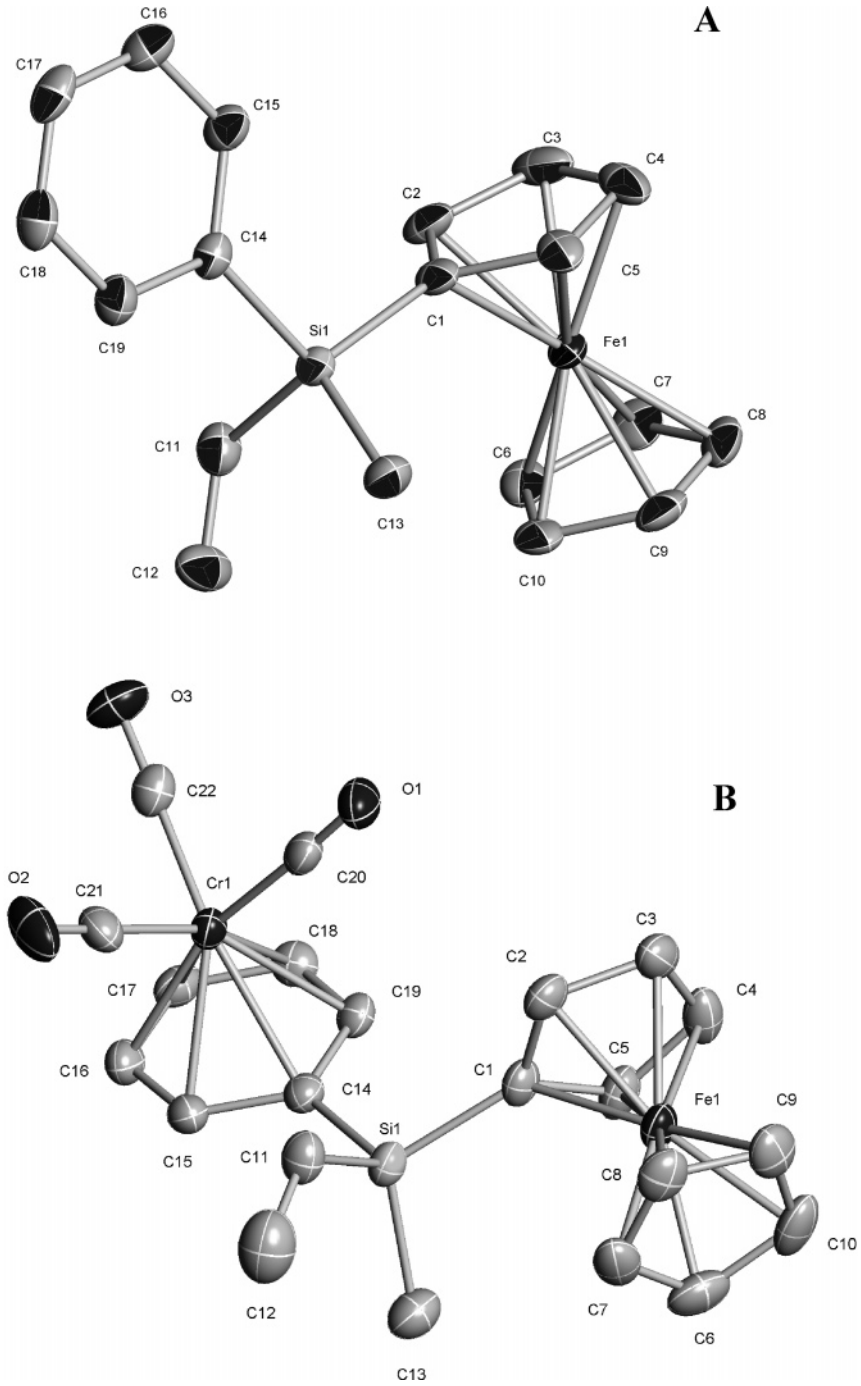

Figure 1. Molecular structures of **1** (A) and of the heterometallic **4** (B). Hydrogen atoms have been omitted for clarity.

derivatives **1** and **3**. In addition, resonances at ca. δ 233 ppm due to the carbonyl carbon atoms were observed in the ^{13}C NMR spectra of **4** and **5**. The ^{29}Si NMR spectra of these dendritic molecules are of interest, as they exhibit only the signals expected for one (in **1** and **4**) and two (for **3** and **5**) different types of silicon environments present in the molecules. Mass spectral analysis of dendritic wedges **1**, **3**, **4**, and **5** confirmed the targeted dendritic structures. Specifically, in the fast atom bombardment (FAB) mass spectra of the heterometallic **4** and **5**, characteristic consecutive loss of $M^+ - 3CO$ and $M^+ - Cr(CO)_3$ units was detected, in addition to the peak corresponding to the molecular ion M^+ at *m*/*z* 468.1 (for **4**) and *m*/*z* 1221.0 (for **5**).

X-ray Structures of 1 and 4. Single-crystal X-ray diffraction studies of the two vinyl-substituted molecules **1** and **4** were undertaken. Crystals of **1** and **4** were obtained at −40 °C from a solution of the corresponding compound in hexane. Figure 1 shows views of the molecular structures of **1** and **4**. A summary of crystallographic data and data collection parameters is included in Table 1. Table 2 contains a comparison of selected bond lengths and angles of compounds **1** and **4**.

The two ferrocenyl-functionalized silanes **1** and **4** are chiral about the silicon atom, and both form monoclinic crystals with space group $P2_1/c$. In the monometallic **1** there are two different molecules in the unit cell corresponding to the two enantiomers (36.5% and 63.5%, respectively). The phenyl substituent is arranged in an almost perpendicular position relative to the ferrocenyl cyclopentadienyl rings. In the heterometallic **4** the $Cr(CO)_3$ tripod is coordinated in a *transoid* arrangement with respect to the silicon-bridged ferrocenyl moiety. The silicon atoms are nearly tetrahedral, with C−Si−C bond angles of 108.8° (for **1**) and 106.1° (for **4**). The cyclopentadienyl rings

Table 1. Crystal Data and Structure Refinement Details for Compounds 1 and 4

	1	4
empirical formula	$C_{19}H_{18}FeSi$	$C_{22}H_{20}CrFeO_3Si$
fw	330.27	468.32
temp, K		100(2)
wavelength, Å		1.54178
cryst syst		monoclinic
space group		$P2_1/c$
a, Å	7.3569(2)	10.4463(2)
b, Å	12.9056(4)	11.9294(2)
c, Å	17.5057(5)	16.3013(3)
α, deg	90	90
β, deg	100.907(2)	97.0010(10)
γ, deg	90	90
V, Å^3	1632.06(8)	2016.29(6)
Z	4	4
density (calcd), mg m^{-3}	1.344	1.543
abs coeff, mm^{-1}	8.012	10.945
F(000)	688	960
cryst size, mm^3	0.25 × 0.10 × 0.10	0.10 × 0.09 × 0.04
θ , deg	4.28 to 71.32	4.26 to 67.07
index ranges	$-8 \le h \le 7$	$-12 \le h \le 10$
	$-15 \le k \le 14$	$-14 \le k \le 13$
	$20 \le l \le 20$	$-17 \le l \le 18$
no. of reflns collected	17 159	13 231
no. of indep reflns	3083 [R(int) = 0.0322]	3434 [R(int) = 0.0482]
completeness to $\theta = 71.32°$	97.6%	95.5%
absorp corr	semiempirical from equivalents	
refinement method	full-matrix least-squares on F^2	
no. of data/restraints/params	3083/0/200	3434/0/254
goodness-of-fit on F^2	1.063	1.019
final R indices ($I > 2\sigma(I)$)	$R_1 = 0.0290$, $wR_2 = 0.0781$	$R_1 = 0.0412$, $wR_2 = 0.1027$
R indices (all data)	$R_1 = 0.0298$, $wR_2 = 0.0787$	$R_1 = 0.0577$, $wR_2 = 0.1110$
largest diff peak and hole, e Å^{-3}	0.478 and −0.235	0.785 and −0.310

Table 2. Selected Bond Lengths (Å) and Angles (deg) for Compounds 1 and 4

	1	4
Fe(1)−C(1)	2.0534(16)	2.048(3)
Si(1)−C(1)	1.8528(18)	1.853(4)
Si(1)−C(11)	1.8638(19)	1.853(4)
Si(1)−C(13)	1.8695(19)	1.870(4)
Si(1)−C(14)	1.8845(17)	1.894(4)
C(11)−C(12)[a]	1.298(4)	1.320(6)
Cr(1)−C(14)		2.246(3)
Cr(1)−C(20)		1.851(4)
Cr(1)−C(21)		1.840(4)
Cr(1)−C(22)		1.849(4)
Si(1)−C(1)−Fe(1)	125.02(9)	126.34(19)
C(1)−Si(1)−C(11)	109.29(8)	111.08(17)
C(1)−Si(1)−C(13)	110.04(8)	111.92(18)
C(1)−Si(1)−C(14)	108.80(7)	105.91(16
C(11)−Si(1)−C(13)	110.96(9)	110.99(19)
C(12)−C(11)−Si(1)	124.21(19)	108.55(16)
C(13)−Si(1)−C(14)		108.17(17)
C(21)−Cr(1)−C(20)		87.52(16)
C(21)−Cr(1)−C(22)		88.18(17)
C(22)−Cr(1)−C(20)		88.24(17)

[a] For **1** this distance is shorter than for **4** due to the contribution of the disorder of the vinyl group.

of the ferrocenyl moiety in **1** are essentially planar and nearly parallel and exhibit a fully eclipsed conformation. By contrast, the two cyclopentadienyl groups of the heterometallic **4** are arranged in a conformation between eclipsed and staggered, which is presumably due to the sterically demanding $Cr(CO)_3$ tripod coordinated to the phenyl ring. In η^6-arene$Cr(CO)_3$ compounds, the orientation of the carbonyl ligands with respect to the arene substituents has been shown to be dependent on both the donor and steric properties of the substituent.[21] In the heterobimetallic **4** the $Cr(CO)_3$ tripod adopts a nearly staggered *exo* conformation with similar Cr−C_{arene} and Cr−CO bond distances that compare well with those found for related $Cr(CO)_3$-containing compounds.[22]

The molecular arrangement of **4** in the crystal structure shown in Figure 2 is of interest. An examination of the crystal packing diagram along the *c*-axis shows that association of similar organometallic moieties, a type of self-assembly, is apparently driving the packing in the crystal. The intermolecular chromium distances to the next neighboring molecules range between 6.206 and 8.487 Å and place the $Cr(CO)_3$ tripods in a favorable proximity for cluster-forming intermolecular solid-state reactions. Thus, one can clearly observe repeating chromium-rich and ferrocene-rich layers lying in the *ab*-plane; the distance between one of these Fe pseudolayers to the Cr neighbor one is 4.0318 Å.

Synthesis of the Homo- and Heterometallic Dendrimers 7−10. In the convergent approach, the previously synthesized dendritic wedges are attached to a multifunctional core unit in the final steps of the dendrimer construction.[16,17] In this work, the availability of free olefinic substituents at the focal point of the dendritic wedges **1**, **3**, **4**, and **5**, potentially enables their attachment to many different Si−H functionalized cores via hydrosilylation chemistry. The four-directional carbosilane Si$[(CH_2)_3Si(Me)_2H]_4$ (**6**), in which the reactive Si−H are located at the end of quite long silicon-containing chains, was selected as a dendritic core, in order to prevent the possibility of steric congestion and provide the final dendrimers with a fourth branched core. Having obtained two different key starting vinyl-functionalized molecules **1** and **4**, the two synthetic pathways

(21) Davis, R.; Kane-Maguire, L.A. P. In *Comprehensive Organometallic Chemistry*; Wilkinson, G., Stone, F. G. A., Abel, E. W., Eds.; Pergamon: Oxford, England, 1982; Vol. 3, pp 1001−54.

(22) See for example: (a) Santi, S.; Ceccon, A.; Bisello, A.; Durante, C.; Ganis, P.; Orian, L. *Organometallics* **2005**, *24*, 4691. (b) Gomes, E. L. S.; Hörner, M.; Young, V. G., Jr.; Dupont, J.; Caliman, V.; Casagrande, O. L., Jr. *Organometallics* **1999**, *18*, 3869. (c) Müller, T. J. J.; Blümel, J. *J. Organomet. Chem.* **2003**, *683*, 354.

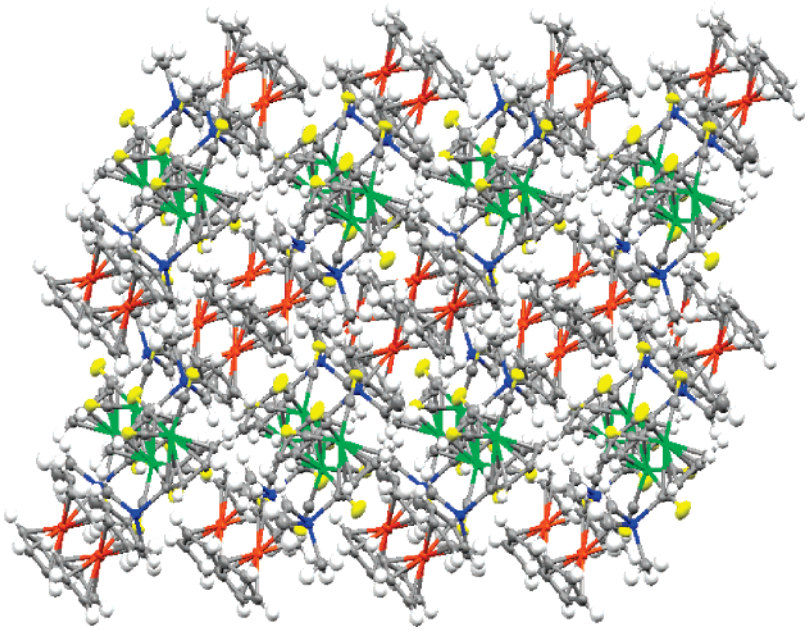

Figure 2. Crystal-packing diagram of **4** showing the iron-rich and chromium-rich pseudolayers.

depicted in Scheme 2 can be envisaged to obtain the targeted first-generation heterooctametallic dendrimer **7**, and both were attempted.

The two routes that were employed to prepare dendrimer **7** involve either (A) hydrosilylation reaction of the heterobimetallic **4** with the carbosilane core **6** or (B) synthesis of the first-generation tetraferrocenyl dendrimer **8**, by hydrosilylation reaction of **1** and **6**, followed by thermal treatment of **8** with chromium hexacarbonyl. Route A has the advantage that the desired heterometallic dendrimer **7** is produced directly, in a single hydrosilylation reaction step after chromium complexation of the phenyl ring to $Cr(CO)_3$ units in **4**. However, attempts to graft by hydrosilylation reaction the $Cr(CO)_3$-complexed dendritic wedge **4** to the core molecule **6** failed in large measure to afford the expected heterooctametallic dendrimer **7**. Reaction of **4** with **6**, in toluene at 70 °C, in the presence of Karstedt's catalyst led to significant amount of the starting **4**, in addition to a small amount of the desired **7** and other presumably decomposition materials as inferred from ^{1}H NMR and IR spectra. This result indicates that the presence of the $Cr(CO)_3$ moiety in **4** induces an electron-deficient character on the phenyl ring bound to the Si−CH=CH_2 group that clearly decreases the effectiveness of the hydrosilylation reaction with the Si−H functionalized core molecule **6**.[23−25] Furthermore, isolation of the pure dendrimer **7** from this multicomponent mixture proved to be a very difficult task. Consequently, for further synthetic studies this path to the desired heterometallic dendrimers did not seem very promising and was therefore abandoned.

In route B the hydrosilylation reaction of the Si−CH=CH_2 group with the core **6** was done prior to the coordination of the phenyl ligand to the tricarbonylchromium fragment. This route involves two reaction steps and allowed the synthesis of both the first-generation tetraferrocenyl dendrimer **8** and the targeted heterooctametallic first-generation dendrimer **7**. In contrast to the above-described results, the hydrosilylation reaction of the more electron-rich vinyl-substitued **1** with the Si−H tetrafunctionalized dendrimer **6**, in the presence of Karstedt's catalyst, in toluene solution at 40 °C, proceeded cleanly to completion, affording the first-generation dendrimer **8** (Scheme 2). In the same way, the second-generation octaferrocenyl dendrimer **9** (Chart 1) was synthesized by hydrosilylation reaction of the growth dendritic wedge **3** and the carbosilane core **6**. Again, ^{1}H NMR and IR spectroscopies established that complete reaction of the four Si−H functionalities in **6** was easily achieved under mild conditions. After purification of the hydrosilylated products by column chromatography, the tetraferrocenyl and octaferrocenyl dendrimers **8** and **9** were isolated as air-stable, orange, tacky oils. Subsequent thermal treatment of dendrimers **8** and **9** with $Cr(CO)_6$ in *n*-Bu_2O/THF afforded the desired first- and second-generation heterometallic dendrimers **7** and **10** (see Scheme 2 and Chart 1, respectively). Not surprisingly, thermal displacement of CO in $Cr(CO)_6$ by the phenyl rings of dendrimer **9** was not as facile as with **8**, and more forcing conditions than those used in the synthesis of the octametallic dendrimer **7** were required. After appropriate workup, the desired heterometallic dendrimers **7** and **10**, containing eight and 20 organometallic units, respectively, were isolated as yellow-orange, tacky oils.

The structural identities of the novel ferrocenyl dendrimers **8** and **9** and of the heterometallic dendrimers **7** and **10** were confirmed by IR, ^{1}H, ^{13}C, and ^{29}Si NMR spectroscopies, matrix-assisted laser desorption, ionization time-of-flight mass spectrometry (MALDI-TOF-MS), and elemental analysis. In the ^{1}H NMR spectra of **8** and **9**, confirming evidence for the complete functionalization of the four reactive Si−H sites in the carbosilane dendritic framework **6** with silicon-bridged phenyl and ferrocenyl moieties is provided by the total absence of the Si−H resonance near δ 3.8 ppm, as well as by the expected integration ratio of the protons corresponding to the ferrocenyl groups, the methylene units, and the methyl groups of the carbosilane dendritic framework. The structures of dendrimers **7**−**10** were corroborated by mass spectrometry (FAB or MALDI-TOF). The

(23) It is well-known that electron-withdrawing substituents on the vinyl group decrease the rate of hydrosilylation processes compared to the more electron-donating groups. On the other hand, steric factors due to substituents in both silane and vinyl groups may also affect the rate and completeness of hydrosilylation reactions. See, for example, refs 20, 24, and 25.

(24) (a) Stein, J.; Lewis, L. N.; Smith, K. A.; Lettko, K. X. *J. Inorg. Organomet. Polym.* **1991**, *1*, 325. (b) Liu, H. Q.; Harrod, J. F. *Can. J. Chem.* **1990**, *68*, 1100.

(25) For a recent interesting work illustrating the effect of the substituents of the Si−H and C=C groups on hydrosilylation reactions see: Hilf, S.; Cyr, P. W.; Rieder, D. A.; Manners, I.; Ishida, T.; Chujo, Y. *Macromol. Rapid Commun.* **2005**, *26*, 950.

Scheme 2. Two Alternative Synthetic Routes for the Construction of the Heterometallic Dendrimer 7

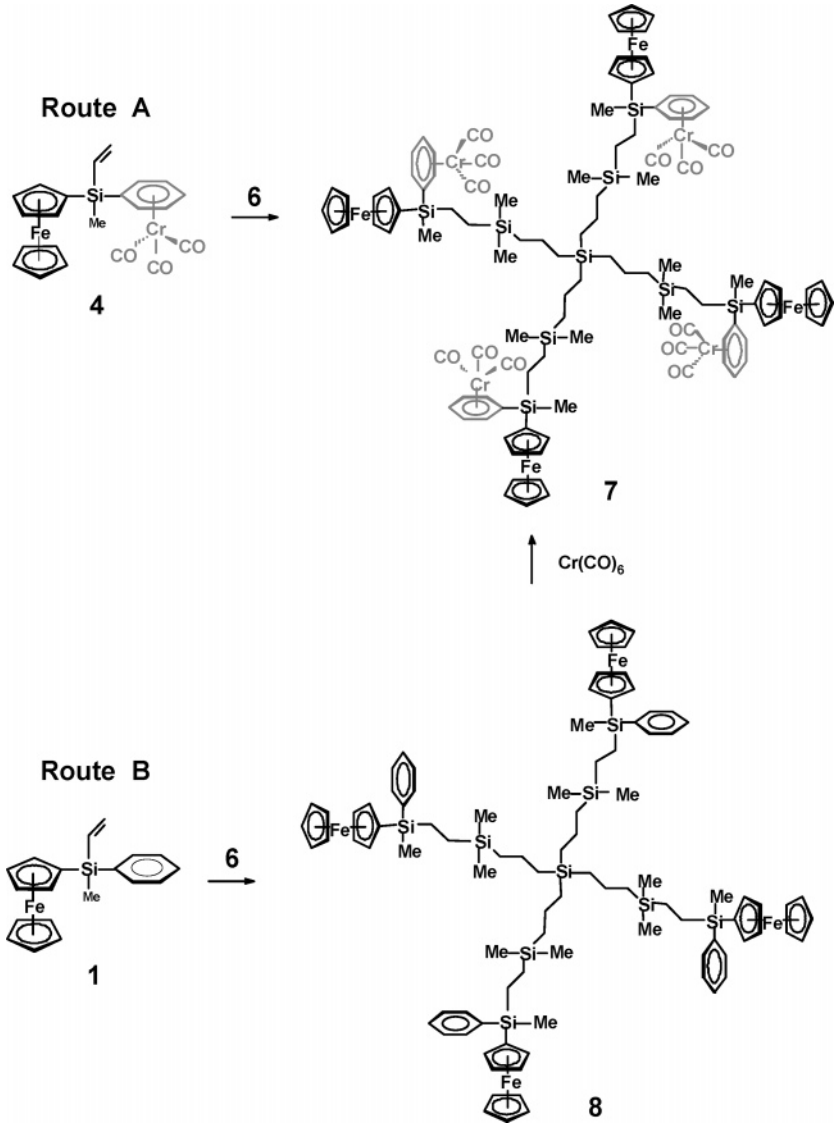

Chart 1

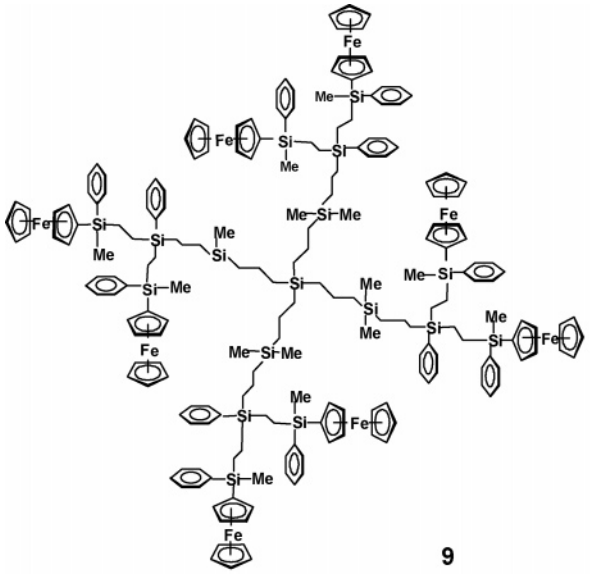

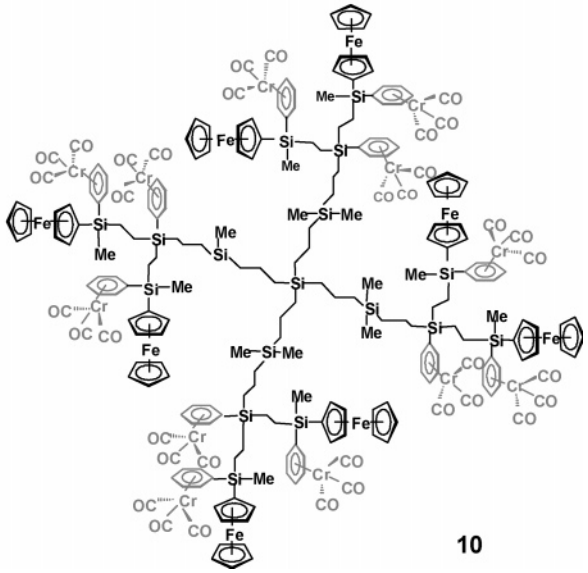

main peaks in the spectra of the tetra- and octanuclear dendrimers **8** and **9** are singly charged molecular ions at *m*/*z* 1761.7 (FAB) and 3684.3 (MALDI-TOF), respectively, which in both cases correspond to the correct molecular mass. The FAB mass spectrum of the heterometallic **7** shows the molecular ion M^+ at *m*/*z* 2304.5 as well as a clear characteristic pattern

Table 3. Cyclic Voltammetric Data for the Homometallic and Heterometallic Dendritic Compounds[a]

compound	Fe centered $E_{1/2}$ (V)[b]	Cr centered $E_{1/2}$ (V)[b]
1	0.44 [0.79]	
3	0.46 [0.83]	
4	0.50 [0.96]	0.90 [0.55]
5	0.52 [1.00]	0.91 [1.10]
7	0.51 [0.97]	0.92 [0.60]
8	0.44 [0.80]	
9	0.45 [0.50]	
10	0.53 [1.05]	0.95 [1.13]

[a] Measured in CH_2Cl_2 solution, $\upsilon = 0.1$ V s^{-1}. [b] The peak potential separation values, ΔE (V), are indicated in brackets.

of peaks that arise from species formed by consecutive loss of $Cr(CO)_3$ moieties (see Supporting Information). In the MALDI-TOF spectrum of dendrimer **10** the molecular ion peak at *m*/*z* 5317.0 is detectable but is much less intense than peaks that arise from the dendrimer minus CO and $Cr(CO)_3$ losses.

Electrochemical Behavior of the Ferrocenyl Dendritic Molecules 1, 3, 8, and 9. An important aspect of this work is to evaluate the redox properties of the new multimetallic dendritic molecules, not only in homogeneous solution but also confined onto electrode surfaces (i.e., where the molecules serve as electrode modifiers). Electrochemical data for the homometallic compounds **1**, **3**, **8**, and **9** are shown in Table 3, together with those of the related heterometallic dendritic molecules.

The cyclic voltammograms (CVs) of **1**, **3**, **8**, and **9** show a single reversible oxidation process. The voltammetric features (i_{pc}/i_{pa} essentially equal to one unit, ΔE_{pk} values about 50−85 mV, and E_{pk} independent of the scan rate) clearly show that the oxidation of **1** and **3** and of the dendrimers **8** and **9** is chemically and electrochemically reversible, resulting in the production of the ferricinium species $[\mathbf{1}]^+$ and the stable and soluble polycations $[\mathbf{3}]^{2+}$, $[\mathbf{8}]^{4+}$, and $[\mathbf{9}]^{8+}$. Coulometry measuments in CH_2Cl_2 solutions indicated the removal of one (for **1**), two (for **3**), four (for **8**), and eight (for **9**) electrons/molecule. In addition, differential pulse voltammetry measurements (DPV) gave only one wave (see Supporting Information), indicating that the oxidation of all the ferrocenyl moieties in the dendritic molecules occurs at the same potential. The electrochemical results unequivocally demonstrate that in the polyferrocenyl dendrimers **8** and **9** the observed reversible oxidation waves represent a simultaneous multielectron transfer of four and eight electrons, respectively, as expected for independent, reversible one-electron process, at the same potential, of the four (in **8**) and eight (in **9**) noninteracting ferrocenyl redox centers.[26]

On the other hand, the diffusion coefficients (D_o) for the polyferrocenyl dendrimers in CH_2Cl_2 solution have been calculated from cyclic voltammetry using the Randles−Sevcik equation.[27] As expected, the diffusion coefficients of the multimetallic dendritic molecules **8** and **9** ($D_o = 4.13 \times 10^{-6}$ and 6.57×10^{-7} cm^2 s^{-1}, respectively) are lower than that of the monometallic **1** ($D_o = 6.92 \times 10^{-6}$ cm^2 s^{-1}) of small size. Furthermore, the values of the diffusion coefficients increase as the number of peripheral ferrocenyl moieties increases; that is, D_o increases with increasing dendrimer generation.

A key feature concerning the ferrocenyl dendrimers **8** and **9** is their ability to deposit onto electrode surfaces as they become oxidized. Thus, modification of electrodes with films of dendrimers **8** and **9** containing, respectively, reversible four- and eight-electron redox systems has been successful, resulting in detectable electroactive material persistently attached to the electrode surfaces. The voltammetric response of an electrodeposited film of the second-generation dendrimer **9** in CH_2Cl_2 is shown in Figure 3, as an illustrative example. The electroactive dendrimer film behaved almost ideally with rapid electron- and charge-transfer kinetics.

A well-defined, symmetrical oxidation−reduction wave is observed, which is characteristic of a surface-confined redox couple, with the expected linear relationship of peak current with potential sweep rate υ (see inset in Figure 3).[28] The shape of the features in the cyclic voltammograms is independent of the scan rate from 5 to 1000 mV s^{-1}, and repeated scanning does not change the voltammograms, demonstrating that films of the octaferrocenyl **9** are stable to electrochemical cycling. A formal potential value of $E_{1/2} = +0.45$ V vs SCE was found for films of **9**, which is nearly identical to the formal potential of the octametallic dendrimer **9** in solution. For films examined at scan rates lower than 100 mV s^{-1} no splitting between the oxidation and reduction peaks was observed, and ΔE_{pk} increases only slightly with increasing sweep rate ($\Delta E_{pk} = 15$ mV at 150 mV s^{-1}), suggesting that the rate of electron transfer is rapid on the experimental time scale. Likewise, a value of the full width at half-maximum, ΔE_{fwhm}, of 58 mV was measured for the surface wave (at a scan rate of 100 mV s^{-1}), which is smaller than the ideal peak width expected for surface-confined redox species,[29] indicating that attractive interactions take place between the electroactive ferrocenyl sites attached to the electrode surface.[28] Noteworthy, Pt and glassy-carbon electrodes modified with films of **9** are extremely durable and reproducible. Extended cyclic voltammetric scans can be carried out in CH_2Cl_2 and CH_3CN solutions with no detectable loss of electrodeposited material. This is an important observation since many of the potential applications of the modified electrodes as multielectron-transfer mediators will require extensive redox cycling. Electrodeposited films of the tetraferrocenyl first-generation dendrimer **8**, obtained under the same conditions as for **9**, showed qualitatively similar voltammetric responses and a comparable stability to the redox process.

Electrochemistry of the Heterometallic Dendritic Molecules 4, 5, 7, and 10. The electrochemical oxidation of **4**, **5**, **7**, and **10** has been examined by cyclic voltammetry and differential pulse voltammetry using CH_2Cl_2 as non-nucleophilic solvent and *n*-Bu_4NPF_6 as supporting electrolyte. The electrochemical behavior of these dendritic molecules is in accordance with their heterometallic nature. For the bimetallic **4** and the octametallic **7** the voltammetric behavior of the two molecules is quite analogous, and the CV for dendrimer **7** is illustrated in Figure 4 as an example.

Scanning up to the potential of 1.20 V vs SCE, the cyclic voltammogram of **7** reveals two diffusion-controlled, reversible oxidation processes at about $E_{1/2} = 0.51$ V and $E_{1/2} = 0.93$ V vs SCE, respectively (see data in Table 3). The first oxidation process can be ascribed to the oxidation of the iron centers, and the second one to the oxidation of the chromium centers. For both heterometallic compounds **4** and **7**, the $E_{1/2}$ values of the first oxidation process are slightly higher than the $E_{1/2}$ found for the oxidation of the iron centers of the related homometallic

(26) Flanagan, J. B.; Margel, S.; Bard, A. J.; Anson, F. C. *J. Am. Chem. Soc*. **1978**, *100*, 4248.

(27) *Analytical Electrochemistry*, 2 ed.; Wang, J., Ed.; Wiley-VCH: New York, 2000.

(28) (a) Murray, R. W. In *Molecular Design of Electrode Surfaces*; Murray, R. W., Ed.; Techniques of Chemistry XXII; Wiley: New York, 1992. (b) Abruña, H. D. In *Electroresponsive Molecular and Polymeric Systems*; Skotheim, T. A., Ed.; Dekker: New York, 1988; Vol. 1.

(29) In surface-immobilized redox species, the peak width for an ideal surface wave is $E_{FWHM} = 90.6/n$ (n = number of electrons transferred per molecule). See ref 28.

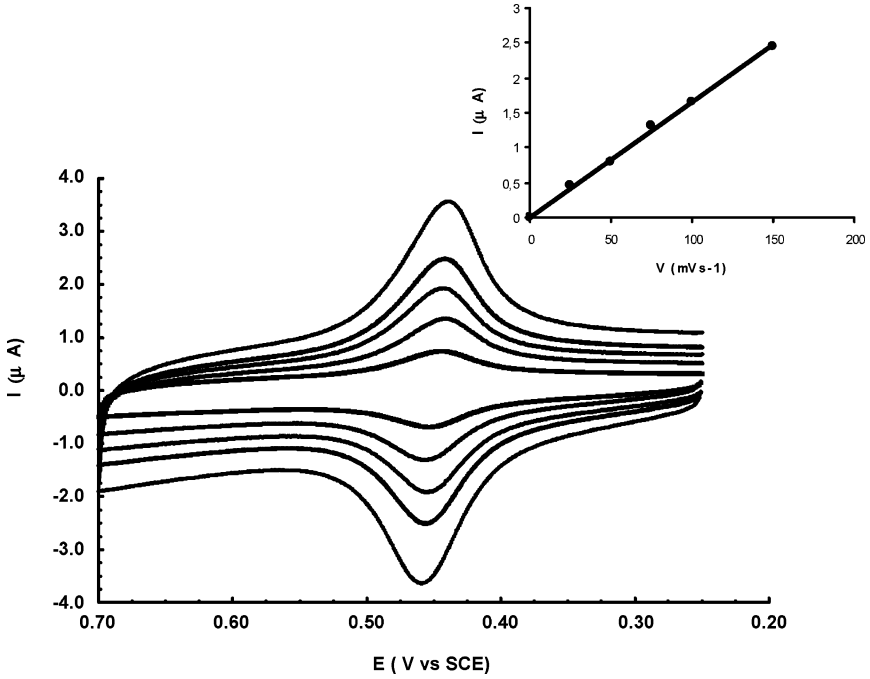

Figure 3. Voltammetric response of a glassy-carbon disk electrode modified with a film of the octaferrocenyl dendrimer **9**, measured in CH_2Cl_2 with 0.1 M *n*-Bu_4NPF_6. Scan rates: 25, 50, 75, 100, and 150 mV s^{-1}. Inset: Scan rate dependence of the anodic peak current. The surface electroactive coverage of ferrocenyl sites in the film was $\Gamma = 2.11 \times 10^{-10}$ mol of ferrocenyl sites cm^{-2}.

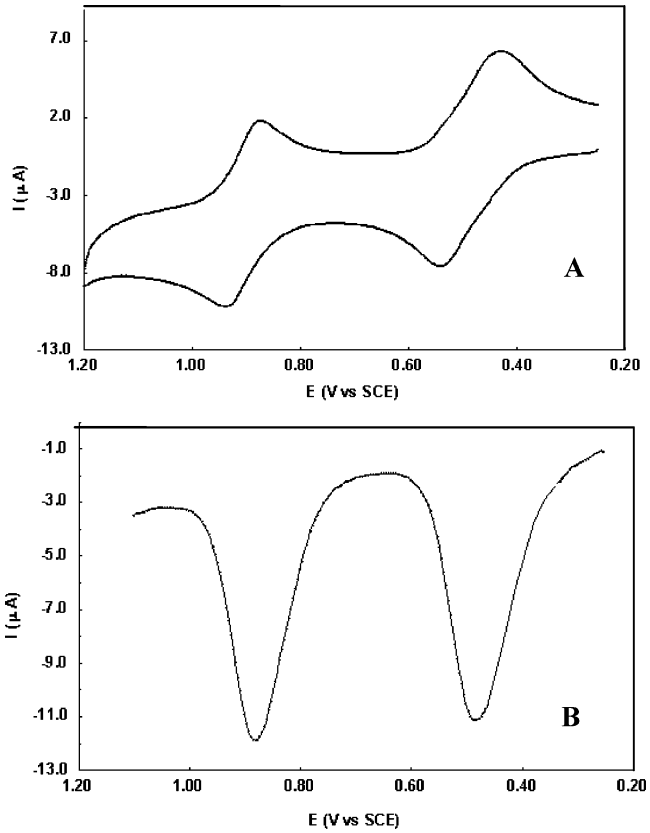

Figure 4. Cyclic voltammogram (A) and differential pulse voltammogram (B) of **7** in CH_2Cl_2 solution.

ferrocenyl precursor molecules **1** and **8**, and this is reasonably due to the electron-withdrawing nature of the adjacent (η^6-C_6H_5)$Cr(CO)_3$ moieties, bonded through a bridging silicon atom. In addition, the chromium-centered oxidations of the heterometallic **4** and **7** show a slight anodic shift with respect to the $E_{1/2}$ for (η^6-C_6H_5)$Cr(CO)_3$ as a result of the positive charges in $[\mathbf{4}]^+$ and $[\mathbf{7}]^{4+}$ generated after the first oxidation process.

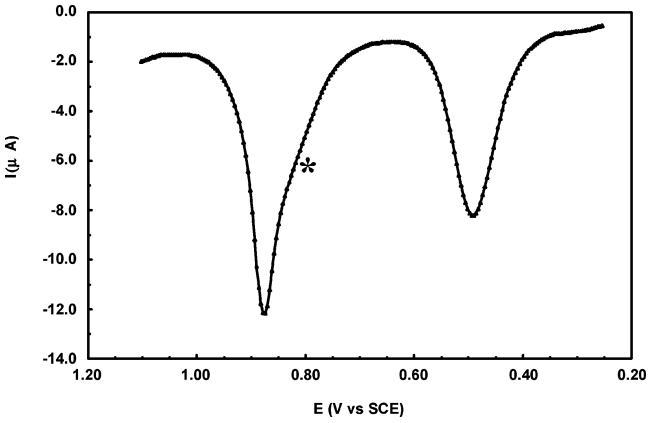

Figure 5. Differential pulse voltammogram of the pentametallic **5** in CH_2Cl_2/*n*-Bu_4NPF_6 solution.

The pentametallic dendritic wedge **5**, which has two ferrocenyl moieties and three (η^6-aryl) cromiumtricabonyl subunits, shows a somewhat different electrochemical oxidation voltammetric feature. The presence of an extra (η^6-C_6H_5)$Cr(CO)_3$ moiety, nonbonded to a ferrocenyl unit, is naturally reflected by an additional chromium-centered oxidation process. The cyclic voltammogram of the pentametallic **5** in CH_2Cl_2 solution exhibits two separated oxidation waves, the second one being broad and poorly resolved. Both electron transfers exhibit directly associated responses in the reverse scan. For both waves, the ratio of cathodic to anodic peak current (i_{pc}/i_{pa}) was close to unity, and the plot of peak current vs $v^{1/2}$ was linear, indicating diffusion-controlled redox processes. On the other hand, the differential pulse voltammogram of **5** in CH_2Cl_2 solution shown in Figure 5 exhibits two separated peaks of different heights. The second peak is broader than the first and displays a shoulder (marked in Figure 5 with an asterisk), suggesting two overlapped redox processes. Integration of the peak areas gives a first to second wave ratio of 2:3. Formal potentials were calculated from the DPV peak potentials, and the results obtained were $E_{1/2} =$ 0.51 V for the process corresponding to the first peak, $E_{1/2} \approx$

0.80 V for the second peak (observed as a shoulder), and $E_{1/2} = 0.91$ V for the peak at higher potential.

Assignment of the formal potentials observed in the DPV of **5** to the corresponding electrochemical processes has been carried out by comparison with the redox potentials observed for the related dendritic homo- and heretometallic dendritic molecules **3** and **4**, respectively. On this basis, it looks reasonable to suggest that the two ferrocenyl moieties of **5** are the first metallic centers to be oxidized. Consequently, the first oxidation peak is attributed to the simultaneous two-electron transfer of two electrons removed from the two ferrocenyl subunits in the molecule, resulting in the formation of the dicationic species $[\mathbf{5}]^{2+}$. The central, almost unresolvable, oxidation peak (at about $E_{1/2} = 0.80$ V) presumably is centered in the chromium center of the isolated (η^6-C_6H_5)$Cr(CO)_3$ unit linked to the Si-allyl group. Finally, two electrons are removed (at $E_{1/2} = 0.91$ V) from the remaining chromium centers of the (η^6-C_6H_5)$Cr(CO)_3$ moieties neighboring the ferrocenyl moieties already oxidized. The heterometallic dendrimer **10** displayed a qualitatively similar DPV response, although in this case the second oxidation wave was considerably broadened and the redox process displays electrochemical irreversibility, as shown by the absence of the corresponding cathodic peak in the reverse scan.

Concluding Remarks

We have designed and explored an efficient convergent growth approach that permits the preparation of a new family of redox-active heterometallic dendritic molecules, derived from carbosilane frameworks and functionalized with silicon-linked ferrocenyl and (η^6-C_6H_5)$Cr(CO)_3$ moieties. In this synthetic strategy suitable organometallic dendritic wedges containing a single olefinic functionality at the focal point are constructed first. Subsequently, these dendrons are attached to a Si−H tetrafunctionalized core molecule via hydrosilylation chemistry in order to provide the final first- and second-generation heterometallic dendrimers with a fourth branched core. The convergent methodology described here is advantageous because of its simplicity and offers ample opportunities for structural variations; therefore, it will represent a versatile method for accessing a potentially large number of dendritic molecules containing organometallic moieties of different nature. Further extension of this synthetic aproach is in progress in order to prepare siloxane-based heterometallic dendritic polymeric assemblies (dendronized polymers).[30]

Experimental Section

Materials and Equipment. All reactions and compound manipulations were performed under an oxygen- and moisture-free atmosphere (N_2 or Ar) using standard Schlenk techniques. Solvents were dried by standard procedures over the appropriate drying agents and distilled immediately prior to use. Ferrocene and $Cr(CO)_6$ (Fluka) were purified by sublimation prior to use. *tert*-Butyllithium (1.7 M solution in pentane), *n*-butyllithium (2.5 M solution in hexane), allylmagnesium bromide (1.0 M solution in diethyl ether), and tetraallylsilane (Aldrich) were used as received. (Tri-*n*-butylstannyl) chloride (Aldrich) and methylphenylvinylchlorosilane (Fluka) were distilled prior to use. Platinum-divinyltetramethyldisiloxane complex (3−3.5% in xylene) (Karstedt's catalyst), available from Petrarch Systems Inc., was used as received. Silica gel (70−230 mesh) (Merck) was used for column chromatographic purifications. (Tri-*n*-butylstannyl)ferrocene was synthesized as described in the literature.[19] Phenylchlorosilane was prepared by reaction of phenylsilane (Fluka) with PCl_5 according to the literature.[31] The carbosilane $Si[(CH_2)_3SiMe_2H]_4$ (**6**) was prepared by treatment of $Si[(CH_2)_3SiMe_2Cl]_4$ with $LiAlH_4$, as we have described previously.[14] Infrared spectra were recorded on a Bomem MB-100 FT-IR spectrometer. NMR spectra were recorded on Brucker-AMX-300 and Bruker DRX-500 spectrometers. Chemical shifts are reported in parts per million (δ) with reference to residual solvent resonances for ^1H and ^{13}C NMR ($CDCl_3$, ^1H, δ 7.27 ppm; ^{13}C, δ 77.0 ppm). ^{29}Si NMR spectra were recorded with inverse-gated proton decoupling in order to minimize nuclear Overhauser effects. In some cases the solutions contained 0.015 M $Cr(acac)_3$ in order to reduce T1's. FAB mass spectral analyses were conducted on a VG Auto Spec mass spectrometer equipped with a cesium ion gun. The MALDI-TOF mass spectra were obtained using a Reflex III (Bruker) mass spectrometer equipped with a nitrogen laser emitting at 337 nm. The matrix was ditranol. Elemental analyses were performed by the Microanalytical Laboratory, Universidad Autónoma de Madrid, Madrid, Spain.

Electrochemical Measurements. Cyclic voltammetric experiments were recorded on a BAS-CV-50W potentiostat. CH_2Cl_2 (spectrograde) for electrochemical measurements was freshly distilled from calcium hydride under argon. The supporting electrolyte was tetra-*n*-butylammonium hexafluorophosphate (Fluka), which was purified by recrystallization from ethanol and was typically used at a concentration of 0.1 M. A conventional three-electrode cell connected to an atmosphere of prepurified nitrogen was used. All cyclic voltammetric experiments were performed using either a platinum-disk working electrode ($A = 0.020$ cm^2) or a glassy carbon-disk working electrode ($A = 0.070$ cm^2). All potentials are referenced to the saturated calomel electrode (SCE). A coiled platinum wire was used as a counter electrode. Solutions were typically 10^{-4} to 10^{-3} M in the redox-active species for cyclic voltammetry. The solutions for the electrochemical experiments were purged with nitrogen and kept under an inert atmosphere throughout the measurements. Differential pulse voltammetry was done with scan rates of 20 and 50 mV s^{-1}, a pulse height of 50 mV, duration of 50 ms, and pulse intervals of 2 s. Formal potentials were calculated from the DPV peak potentials using $E_{1/2} = E_{pk} + E_{pulse}/2$, where E_{pulse} is the pulse height. Coulometric measurements were made with a PAR-379 digital coulometer, using Pt gauze as a working electrode.

X-ray Crystal Structure Determination. Compounds **1** and **4** were structurally characterized by single-crystal X-ray diffraction. A suitable orange crystal of **1** of needle shape and dimensions 0.25 × 0.10 × 0.10 mm and a suitable yellow crystal of **4** of star shape and dimensions 0.10 × 0.09 × 0.04 mm were located and mounted on a glass fiber with "magic oil". The samples were transferred to a Bruker SMART 6K CCD area-detector three-circle diffractometer with a MacScience rotating anode (Cu Kα radiation, $\lambda = 1.54178$ Å) generator equipped with Goebel mirrors at settings of 50 kV and 100 mA. For compound **1** a total of 3083 independent reflections ($R_{int} = 0.0322$) were colleted in the range $4.28° < \theta < 71.32°$. For **2** a total of 3434 independent reflections ($R_{int} = 0.0482$) were colleted in the range $4.26° < \theta < 67.07°$. X-ray data were collected at 100 K, with a combination of six runs at different φ and 2θ angles, 3600 frames. The data were collected using 0.3° wide ω scans with a crystal-to-detector distance of 4.0 cm. The substantial redundancy in data allows empirical absorption corrections (SADABS)[32] to be applied using multiple measurements of symmetry-equivalent reflections. The raw intensity data frames were integrated with the SAINT program,[33] which also applied correc-

(30) Further studies of the use of **1** and **4** in the synthesis of siloxane-based heterometallic dendritic and polymeric assemblies are in progress and will be reported.

(31) Mawaziny, S. *J. Chem. Soc. (A)* **1970**, 1641.

(32) Sheldrick, G. M. *SADABS* Version 2.03, Program for Empirical Absorption Correction; University of Göttingen: Germany, 1997−2001.

tions for Lorentz and polarization effects. The software package SHELXTL version 6.10 was used for space group determination, structure solution, and refinement.[34] The space group determination was based on a check of the Laue symmetry and systematic absences and was confirmed using the structure solution. The structures were solved by direct methods (SHELXS-97), completed with difference Fourier syntheses, and refined with full-matrix least-squares using SHELXL-97, minimizing $w(F_o^2 - F_c^2)^2$.[35,36] Weighted R factors (R_w) and all goodness of fit S are based on F^2; conventional R factors (R) are based on F. All non-hydrogen atoms were refined with anisotropic displacement parameters. The hydrogen atom positions were calculated geometrically and were allowed to ride on their parent carbon atoms with fixed isotropic U. All scattering factors and anomalous dispersions factors are contained in the SHELXTL 6.10 program library. The crystal structures of **1** and **4** have been deposited at the Cambridge Crystallographic Data Centre and allocated the deposition numbers CCDC648116 and CCDC 648117, respectively.

Synthesis of (CH_2═CH)MePhSiFc (1). Ferrocenyllithium was generated in situ via the reaction of (tri-*n*-butylstannyl)ferrocene (30.0 g, 63.2 mmol) with *n*-butyllithium (28.5 mL, 2.5 M solution in hexane) in 50 mL of THF at −78 °C. After 90 min, the mixture was warmed to −30 °C. To this stirred system was added dropwise methylphenylvinylchlorosilane (11.30 g, 52.0 mmol) in 20 mL of THF. The mixture was allowed to warm to room temperature and was stirred for 14 h. The solution was concentrated, treated with hexane, and then filtered to remove the lithium chloride byproduct. Solvent removal yielded an orange, oily product, which was purified by column chromatography on silica gel using hexane as eluent. A first band containing ferrocene was eluted and, subsequently, a second major orange band was collected. Solvent removal afforded the desired product **1** as an air-stable, orange, crystalline solid. Yield: 14.50 g (75%). Anal. Calcd for $C_{19}H_{20}SiFe$: C, 68.66; H, 6.07. Found: C, 68.58; H, 6.10. ^{1}H NMR ($CDCl_3$, 300 MHz): δ 0.61 (s, 3H, CH_3), 4.10 (s, 5H, C_5H_5), 4.14, 4.17, 4.40 (m, 4H, C_5H_4), 5.85 (dd, ^3J = 19.8 Hz, ^2J = 3.3 Hz, 1H, CH═CH_{trans} H_{cis}), 6.15 (dd, ^3J = 14.8 Hz, ^2J = 3.3 Hz, 1H, CH═CH_{trans} H_{cis}), 6.40 (dd, ^3J = 19.8 Hz, ^2J = 14.8 Hz, 1H, CH═CH_2), 7.34 (m, 3H, C_6H_5), 7.53 (m, 2H, C_6H_5). ^{13}C{^{1}H} NMR ($CDCl_3$, 75.43 MHz): δ −3.75 (*C*H$_3$), 67.38, 68.32, 71.12, 73.66 (C_5H_5/C_5H_4), 127.61, 128.95, 134.26, 136.84 (C_6H_5), 133.53, 137.70 (*C*H═*C*H$_2$). ^{29}Si{^{1}H} NMR ($CDCl_3$, 59.3 MHz): δ −14.05 (*Si*(CH$_3$)). MS (FAB): *m*/*z* (%): 332.6 [M$^+$], (100), 147.6 [SiMe(CH═*C*H$_2$)]$^+$, (35.2).

Synthesis of PhClSi[$(CH_2)_2$MePhSiFc]$_2$ (2). To a solution of **1** (1.00 g, 3.0 mmol) in toluene (30 mL) was added 40 μL of a solution of Karstedt's catalyst. The mixture was stirred at room temperature for 0.5 h. A solution of phenylchlorosilane (0.20 g, 1.5 mmol) in dry toluene (10 mL) was added dropwise. The mixture was heated to 40 °C, and after a few minutes, a FTIR spectrum of the reaction mixture showed complete loss of the ν(Si−H) absorption at 2179 cm^{-1}. Likewise, ^{1}H NMR spectroscopy confirmed the complete disappearance of the Si−H proton resonances of the starting phenylchlorosilane. The mixture was filtered, the solvent was removed under vacuum, and the remaining orange oil (1.10 g, 95%) was used immediately in the next reaction step. ^{1}H NMR (300 MHz, $CDCl_3$): δ 0.43 (s, 6H, CH_3), 0.92, 1.20 (m, 8H, CH_2CH_2), 4.10 (s, 10H, C_5H_5), 4.08−4.40 (br, 8H, C_5H_4), 7.35, 7.50 (m, 15H, C_6H_5).

Synthesis of (CH_2═CHCH_2)PhSi[$(CH_2)_2$MePhSiFc]$_2$ (3). A solution of 1.10 g (1.42 mmol) of recently prepared **2** in diethyl ether was added dropwise with vigorous stirring to 50 mL of diethyl ether containing 2.0 mL (1.9 mmol) of allylmagnesium bromide (1 M in diethyl ether). The resulting orange solution was refluxed for 4 h, cooled to 0 °C, and then hydrolyzed with aqueous NH_4Cl (10%). The organic layer was separated, washed with water, and dried over anhydrous $MgSO_4$. The solvent was removed under vacuum, and the residue was purified by column chromatography. An orange band was colleted using hexane as eluent. Solvent removal afforded the desired growth dendron **3**, carrying two ferrocenyl units. Yield: 0.70 g (57%). Anal. Calcd for $C_{47}H_{52}Si_3Fe_2$: C, 69.45; H, 6.45. Found: C, 69.38; H, 6.36. ^{1}H NMR ($CDCl_3$, 300 MHz): δ 0.51 (s, 6H, CH_3), 0.83 (m, 8H, CH_2CH_2), 1.83 (d, 2H, CH_2CH═CH_2), 3.99 (s, 10H, C_5H_5), 4.05, 4.10, 4.33 (m, 8H, C_5H_4), 4.82−4.90 (m, 2H, CH═CH_2), 5.75−5.80 (m, 1H, CH═CH_2), 7.35, 7.50 (m, 15H, C_6H_5). ^{13}C{^{1}H} NMR ($CDCl_3$, 75.43 MHz): δ −4.43 (*C*H$_3$), 4.10, 7.78 (*C*H$_2$), 19.69 (*C*H$_2$CH═CH$_2$), 68.39, 69.01, 70.91, 71.08, 73.65, 73.70 (C_5H_4/C_5H_5), 113.6, 134.10 (*C*H═*C*H$_2$), 127.80, 127.91, 129.01, 129.16, 136.30 (C_6H_5). ^{29}Si{^{1}H} NMR ($CDCl_3$, 59.3 MHz): δ −5.15 (*Si*Fc), 0.30 (*Si*CH$_2$CH═CH$_2$). MS (FAB): *m*/*z* (%) 812.0 [M$^+$] (7), 305.0 [SiFcCH$_3$C$_6$H$_5$]$^+$, (100).

Synthesis of (CH_2═CH)MeSi[{(η^6-C_6H_5)Cr(CO)$_3$}Fc] (4). A degassed solution of 0.40 g (1.8 mmol) of chromium hexacarbonyl and 0.50 g (1.5 mmol) of **1** in a mixture of 90 mL of *n*-dibutyl ether and 10 mL of THF was heated to reflux temperature (oil bath 140 °C). Over the course of the reaction, new IR carbonyl bands at 1972 and 1873 cm^{-1} were observed to increase in intensity. Likewise, in the ^{1}H NMR ($CDCl_3$) spectrum, the resonances in the 7.3−7.5 ppm region progressively disappeared while new resonances in the range 5.9−6.5 ppm were detected. After 48 h, the suspension was filtered through a pad of Celite to remove the small amounts of insoluble decomposition products and some unreacted $Cr(CO)_6$. From the resulting light orange solution, the solvent was removed under vacuum, affording a yellow solid, which was purified by treatment with hexane solution at low temperature. After standing at −30 °C, a yellow solid was formed, which was filtered off to afford the desired molecule **4**, which was isolated as an air-unstable, crystalline, yellow solid. Yield: 0.40 g (63%). Anal. Calcd for $C_{22}H_{20}O_3SiFeCr$: C, 56.41; H, 4.31. Found C, 56.30; H, 4.22. ^{1}H NMR ($CDCl_3$, 300 MHz): δ 0.66 (s, 3H, CH_3), 4.14 (s, 5H, C_5H_5), 4.22, 4.23, 4.45 (m, 4H, C_5H_4), 5.09, 5.38, 5.48 (m, 5H, C_6H_5), 5.93 (dd, ^3J = 20.5 Hz, ^2J = 3.6 Hz, 1H, CH═CH_{trans} H_{cis}), 6.24 (dd, ^3J = 15.3 Hz, ^2J = 3.6 Hz, 1H, CH═CH_{trans} H_{cis}), 6.50 (dd, ^3J = 20.5 Hz, ^2J = 15.3 Hz, 1H, CH═CH_2). ^{13}C{^{1}H} NMR ($CDCl_3$, 75.43 MHz): δ −4.11 (*C*H$_3$), 64.42, 68.49, 71.66, 71.84, 73.57 (C_5H_4/C_5H_5), 90.31, 95.73, 97.90, 100.22 (C_6H_5), 134.82 (*C*H═*C*H$_2$), 232.91 (CO). ^{29}Si{^{1}H} NMR ($CDCl_3$, 59.3 MHz): δ −10.88 (*Si*Fc). IR (KBr): ν(C≡O) 1972 and 1873 cm^{-1}. MS (FAB): *m*/*z* (%) 468.1 [M$^+$] (65), 384.1 [M$^+$ − 3CO] (100), 332.1 [M$^+$ − Cr(CO)$_3$], (80).

Synthesis of (CH_2═CHCH_2){(η^6-C_6H_5)Cr(CO)$_3$}Si[$(CH_2)_2$Me-{(η^6-C_6H_5)Cr(CO)$_3$}SiFc]$_2$ (5). Using the same method as detailed for the preparation of **4**, the pentametallic **5** was synthesized starting from 0.57 g (0.7 mmol) of **3** and 0.58 g of $Cr(CO)_6$ (2.6 mmol). The reaction was completed after 72 h as it was established from IR and ^{1}H NMR spectroscopies. The reaction mixture treated as above and the heterometallic dendron **5** was isolated as an air-unstable yellow solid. Yield: (0.21 g, 43%). Anal. Calcd for $C_{56}H_{52}O_9Si_3Fe_2Cr_3$: C, 55.08; H, 4.30. Found: C, 54.96; H, 4.21. ^{1}H NMR ($CDCl_3$, 300 MHz): δ 0.57 (s, 6H, CH_3), 1.02 (br, 8H, CH_2), 1.94 (d, 2H, CH_2CH═CH_2), 4.10, 4.17, 4.45 (m, 18H, C_5H_5/C_5H_4), 4.98, 5.81 (m, 3H, CH═CH_2), 5.13, 5.43, 5.51 (m, 15H, C_6H_5). ^{13}C{^{1}H} NMR ($CDCl_3$, 125.8 MHz): δ −4.87 (Si*C*H$_3$), 4.67, 7.75, (*C*H$_2$*C*H$_2$), 19.29 (*C*H$_2$CH═CH$_2$), 66.08, 68.42, 71.53, 71.72, 73.54 (C_5H_4/C_5H_5), 90.52, 90.77, 95.79, 98.45, 99.75, 100.10, 100.25 (C_6H_5), 115.32, 133.30 (*C*H═*C*H$_2$), 233.10 (*C*O). ^{29}Si{^{1}H} NMR ($CDCl_3$, 99.4 MHz): δ −4.87 (*Si*Fc), 1.03 (*Si*CH$_2$CH═CH$_2$). IR (KBr): ν(C≡O) 1972 and 1873 cm^{-1}. MS (FAB): *m*/*z* (%)

(33) *SAINT+NT* Version 6.04; SAX Area-Detector Integration Program; Bruker Analytical X-ray Instruments: Madison, WI, 1997−2001.

(34) Bruker *AXS SHELXTL* Version 6.10, Structure Determination Package; Bruker Analytical X-ray Instruments: Madison, WI, 2000.

(35) Sheldrick, G. M. *Acta Crystallogr*. *A* **1990**, *46*, 467.

(36) Sheldrick, G. M. *SHELXL97*, Program for Crystal Structure Refinement; Germany, 1997.

1221.0 [M^+] (1), 1084.0 [$M^+ - Cr(CO)_3$] (8), 948.13 [$M^+ - 2Cr(CO)_3$] (4), 812.2 [$M^+ - 3Cr(CO)_3$] (6), 305.0 [$SiFcCH_3C_6H_5$]$^+$ (100).

Synthesis of Dendrimer 7. This heterometallic derivative **7** was obtained by the same thermal procedure as described for **4** and **5**, starting from 0.70 g (0.4 mmol) of **8** and $Cr(CO)_6$ 0.40 g (1.9 mmol). After 72 h the reaction was finished and the residue was treated in a manner similar to **5**. The desired heterometallic dendrimer was isolated as an air-unstable, yellow-orange oil. Yield: 0.32 g (37%). Anal. Calcd for $C_{108}H_{132}Si_9Fe_4O_{12}Cr_4$: C, 56.24; H, 5.77. Found: C, 56.17; H, 5.68. ^{1}H NMR ($CDCl_3$, 300 MHz): δ 0.01 (s, 24H, Si(CH_3)$_2$), 0.56 (m, 12H, CH_3), 0.56 (br, 16H, $CH_2CH_2CH_2$), 0.88 (m, 16H, CH_2), 1.30 (br, 8H, $CH_2CH_2CH_2$), 4.12 (s, 20H, C_5H_5), 4.21, 4.43 (m, 16H, C_5H_4), 5.08, 5.35, 5.47 (m, 20H, C_6H_5). ^{13}C{^{1}H} NMR ($CDCl_3$, 75.43 MHz): δ −4.45 (CH_3), −3.84 (Si(CH_3)$_2$), 8.02, 7.41 (CH_2), 17.51, 18.60, 19.65 ($CH_2CH_2CH_2$), 66.57, 68.34, 71.31, 71.46, 73.48 (C_5H_5/C_5H_4), 90.13, 95.55, 99.15, 100.33 (C_6H_5). ^{29}Si{^{1}H} NMR ($CDCl_3$, 59.3 MHz): δ −1.68 (*Si*Fc), 1.05 (*Si*CH_2), 3.80 (*Si*CH_3)). IR (KBr): ν(C≡O) 1961 and 1882 cm^{-1}. MS (FAB): *m*/*z* (%) 2304.5 [M^+] (11.0), 2170.2 [$M^+ - Cr(CO)_3$] (8), 2035.1 [$M^+ - 2Cr(CO)_3$] (0.5), 1896.7 [$M^+ - 3Cr(CO)_3$] (0.3), 305.1 [$SiFcCH_3C_6H_5$]$^+$ (100).

Synthesis of Dendrimer 8. To a toluene solution (25 mL) of **1** (0.85 g, 2.5 mmol) was added 30 μL of Karstedt's catalyst. The mixture was stirred at room temperature for 0.5 h. A solution of 0.20 g (0.4 mmol) of the carbosilane **6** in toluene was added dropwise, and then the mixture was warmed to 40 °C. The attachment of **1** to the four Si−H active sites of the dendritic core **6** proceeded cleanly to completion in 4 h, as established from ^{1}H NMR and IR analysis of the reaction mixture. The solvent was removed and the resulting oil was subjected to column chromatography using hexane as eluent. A first band containing **1** was separated, and with additional hexane, the desired **8** was eluted. Solvent removal afforded the homometallic dendrimer **8** as an air-stable, orange oil. Yield: 0.73 g (90%). Anal. Calcd for $C_{96}H_{132}Si_9Fe_4$: C, 65.43; H, 7.56. Found: C, 65.28; H, 7.45. ^{1}H NMR ($CDCl_3$, 300 MHz): δ −0.08 (s, 24H, Si(CH_3)$_2$), 0.52 (m, 12H, CH_3), 0.52 (m, 16H, $CH_2CH_2CH_2$), 0.86 (t, 16H, $SiCH_2CH_2$), 1.29 (q, 8H, $CH_2CH_2CH_2$), 4.05 (m, 20H, C_5H_5), 4.10, 4.15, 4.35 (m, 16H, C_5H_4), 7.34 (m, 12H, C_6H_5), 7.53 (m, 8H, C_6H_5). ^{13}C{^{1}H} NMR ($CDCl_3$, 75.46 MHz): δ −4.38 (CH_3), −3.75(Si(CH_3)$_2$), 7.78, 7.91 (CH_2), 17.56, 18.66, 19.75 ($CH_2CH_2CH_2$), 68.32, 69.32, 70.78, 70.94, 73.66 (C_5H_5/C_5H_4), 127.61, 128.945, 134.11, 138.54 (C_6H_5). ^{29}Si{^{1}H} NMR ($CDCl_3$, 59.62 MHz): δ −5.15 (*Si*Fc), 0.73 (*Si*CH_2), 3.56 (*Si*CH_3). MS (FAB): *m*/*z* (%) 1761.7 [M^+] (5), 305.0 [$SiFcCH_3C_6H_5$]$^+$ (100).

Synthesis of Dendrimer 9. This dendrimer was prepared by the same procedure as that described for the synthesis of **8**, starting from 0.42 g (0.5 mmol) of **3** and 0.05 g (0.1 mmol) of **6**. In this case, longer reaction periods (12 h) with a higher temperature (65 °C) were required to achieve the complete incorporation of the growth dendron **3** to the core molecule **6**. After filtration and purification by column chromatography using hexane as eluent, the desired octaferrocenyl dendrimer **9** was isolated as an air-stable, dark orange, tacky oil. Yield: 0.24 g (60%). Anal. Calcd for $C_{208}H_{260}Si_{17}Fe_8$: C, 67.81; H, 7.12. Found: C, 67.65; H, 6.91. ^{1}H NMR ($CDCl_3$, 300 MHz): δ 0.08 (s, 24H, Si(CH_3)$_2$), 0.52 (m, 24H, CH_3), 0.52 (m, 32H, $CH_2CH_2CH_2$), 0.89 (m, 32H, $SiCH_2CH_2$), 1.28 (q, 16H, $CH_2CH_2CH_2$), 4.00 (m, 40H, C_5H_5), 4.06, 4.10, 4.33 (m, 32H, C_5H_4), 7.35, 7.51 (m, 60 H, C_6H_5). ^{13}C{^{1}H} NMR ($CDCl_3$, 125.75 MHz): δ −4.48 (CH_3), −3.12 (Si(CH_3)$_2$), 7.69, 7.73 (CH_2CH_2), 18.45, 20.48 ($CH_2CH_2CH_2$), 68.28, 69.03, 70.79, 70.95, 73.55, 73.60 (C_5H_5/C_5H_4), 127.70, 127.75, 128.81, 128.88, 134.11, 134.29, 138.31 (C_6H_5). ^{29}Si{^{1}H} NMR ($CDCl_3$, 99.36 MHz): δ −5.24 (*Si*Fc), −0.90 (*Si*Ph), 0.95 (*Si*CH_2), 3.46 (*Si*CH_3). MS (MALDI-TOF): *m*/*z* 3684.3 [M^+].

Synthesis of Dendrimer 10. In analogy with the synthesis of **7**, thermal treatment of **9** (0.32 g, 0.08 mmol) with an excess of $Cr(CO)_6$ was carried out during 96 h. After appropriate workup, **10** was isolated as an air-unstable, yellow, tacky oil. Anal. Calcd for $C_{244}H_{260}Si_{17}Fe_8O_{32}Cr_8$: C, 55.12; H, 4.93. Found: C, 54.92; H, 4.74. ^{1}H NMR ($CDCl_3$, 300 MHz): δ 0.06 (br, 24H, Si(CH_3)$_2$), 0.49 (br, 24H, CH_3), 0.49 (br, 32H, $CH_2CH_2CH_2$), 0.90 (m, 32H, CH_2CH_2), 1.31 (br, 16H, $CH_2CH_2CH_2$), 3.90 (s, 40H, C_5H_5), 4.09, 4.34 (br, 32H, C_5H_4), 5.10−5.44 (br, 60H, C_6H_5). ^{13}C{^{1}H} NMR ($CDCl_3$, 125. 75 MHz): δ −4.50 (CH_3), −3.15 (Si(CH_3)$_2$), 7.41, 7.70 (CH_2CH_2), 18.45, 19.95 ($CH_2CH_2CH_2$), 68.19, 69.00, 70.04, 70.90, 72.98, 73.40 (C_5H_5/C_5H_4), 90.50, 95.76, 99.30, 100.20 (C_6H_5). ^{29}Si{^{1}H} NMR ($CDCl_3$, 99.36 MHz): δ −4.83 (*Si*Fc), −3.70 (*Si*Ph), 0.98 (*Si*CH_2), 3.20 (*Si*CH_3)). MS (MALDI-TOF): *m*/*z* 5317.0 [M^+], 5181.0 [$M^+ - Cr(CO)_3$], 5045.0 [$M^+ - 2Cr(CO)_3$], 4909.0 [$M^+ - 3Cr(CO)_3$].

Acknowledgment. The authors thank the Spanish Ministerio de Educación y Ciencia, Projects CTQ2005-02282/BQU and CTQ2004-07381-C01-C02/BQU, for support of this research. We are grateful to Prof. José Losada (Universidad Politécnica de Madrid) for helpful discussions.

Supporting Information Available: Complete crystallographic data for compounds **1** and **4** (CIF files), representative mass spectra for dendrimers **7** (FAB) and **8** (MALDI-TOF), representative CV and DPV figures of ferrocenyl dendrimers, and detailed electrochemical procedure for the modification of electrode surfaces with **8** and **9**. This material is available free of charge via the Internet at http://pubs.acs.org.

OM700559T